

# Comparative expression analysis of *pfdn6a* and *tcp1 $\alpha$* during *Xenopus* development

SILVIA MARRACCI<sup>1</sup>, DAVIDE MARTINI<sup>#,1</sup>, MARTINA GIANNACCINI<sup>#,1,2</sup>, GUIDO GIUDETTI<sup>##,1</sup>, LUCIANA DENTE<sup>1</sup>  
and MASSIMILIANO ANDREAZZOLI<sup>\*,1</sup>

<sup>1</sup>Unità di Biologia Cellulare e dello Sviluppo, Dipartimento di Biologia, Università di Pisa and  
<sup>2</sup>Istituto di Scienze della Vita, Scuola Superiore Sant'Anna, Pisa, Italy

**ABSTRACT** We recently identified *pfdn6a* and *tcp1 $\alpha$*  (also known as *cct- $\alpha$* ) as genes coregulated by the transcription factor Rx1. The proteins encoded by these genes belong to two interacting complexes (Prefoldin and "chaperonin containing t-complex polypeptide 1"), which promote the folding of actin and tubulin and have more recently been reported to be involved in a variety of additional functions including cell cycle control and transcription regulation. However, little is known about the expression and function of these two genes during vertebrate development. To assess whether *pfdn6a* and *tcp1 $\alpha$*  display a general coordinated expression during *Xenopus* development, we determined, by RT-PCR and *in situ* hybridization, the spatio-temporal expression pattern of *pfdn6a*, which was not previously described, and compared it to that of *tcp1 $\alpha$* , extending the analysis to stages not previously investigated for this gene. We detected maternal transcripts of *pfdn6a* in the animal hemisphere at early blastula stage. During gastrulation, *pfdn6a* was expressed in the involuting mesoderm and subsequently in the anterior and dorsal neural plate. At tailbud and tadpole stages, *pfdn6a* RNA was mainly detected in the forebrain, midbrain, eye vesicle, otic vesicle, branchial arches, and developing pronephros. The *pfdn6a* expression pattern largely overlaps with that of *tcp1 $\alpha$*  indicating a spatio-temporal transcriptional coregulation of these genes in the majority of their expression sites, which is suggestive of a possible involvement in the same developmental events.

**KEY WORDS:** *pfdn6*, *hke2*, *tcp1*, *cct*, *Xenopus embryogenesis*

Molecules linking and coordinating cytoskeletal dynamics and gene expression are of particular interest as they play crucial roles in many aspects of a cell's life. A growing number of proteins appears to belong to this class and a recent example is represented by Prefoldin (PFDN), a cochaperone that cooperates with the chaperonin TCP1 (also known as CCT, chaperonin containing tailless complex polypeptide 1), which was shown to operate both in the cytoplasm and in the nucleus (Millan-Zambrano and Chavez, 2014). The function originally described for eukaryotic PFDN, a heterohexameric complex assembled from six different subunits (two different  $\alpha$  and four different  $\beta$  subunits), is to promote the folding of actin and tubulin through the interaction with TCP1, a complex assembled from two stacked rings, each composed of eight different but related subunits (CCT $\alpha$ ,  $\beta$ ,  $\gamma$ ,  $\delta$ ,  $\epsilon$ ,  $\zeta$ ,  $\eta$ ,  $\theta$  in mammals and CCT1–8 in yeast) (Hansen *et al.*, 1999; Martín-Benito *et al.*, 2002). However, a large body of evidence has recently indicated

that PFDN and TCP1 carry out additional functions including control of cell cycle, protein degradation and transcription, as well as exerting protective effects against the accumulation of aggregated proteins, such as pathogenic huntingtin and amyloid- $\beta$  (Pejanovic *et al.*, 2012; Millan-Zambrano and Chavez, 2014).

Functional experiments have shown a central role played by PFDN and TCP1 also during metazoan development. In *Caenorhabditis elegans*, RNAi screens indicate that knockdown of individual PFDN or TCP1 subunits causes morphological abnormalities and variably penetrant embryonic lethal phenotypes, suggesting that these proteins are required for multiple tissue development and embryonic viability (Sönnichsen *et al.*, 2005). In *Drosophila*, mutations in the PFDN3 homologue *mgr* cause reduced tubulin synthesis in somatic and germinal cells, leading to mitotic and

*Abbreviations used in this paper:* PFDN, prefoldin.

\*Address correspondence to: Massimiliano Andreazzoli, Unità di Biologia Cellulare e dello Sviluppo, SS12 Abetone e Brennero, 56127 Pisa, Italy. Tel. +39-050-2211485. Fax + 39-050-2211495 E-mail: massimiliano.andreazzoli@unipi.it

#Note: These authors equally contributed to this work.

##Present address: Scuola Superiore Sant'Anna, The BioRobotics Institute, Translational Neural Engineering Group. 56025 Pontedera (Pisa), Italy.

Accepted: 5 March 2015.

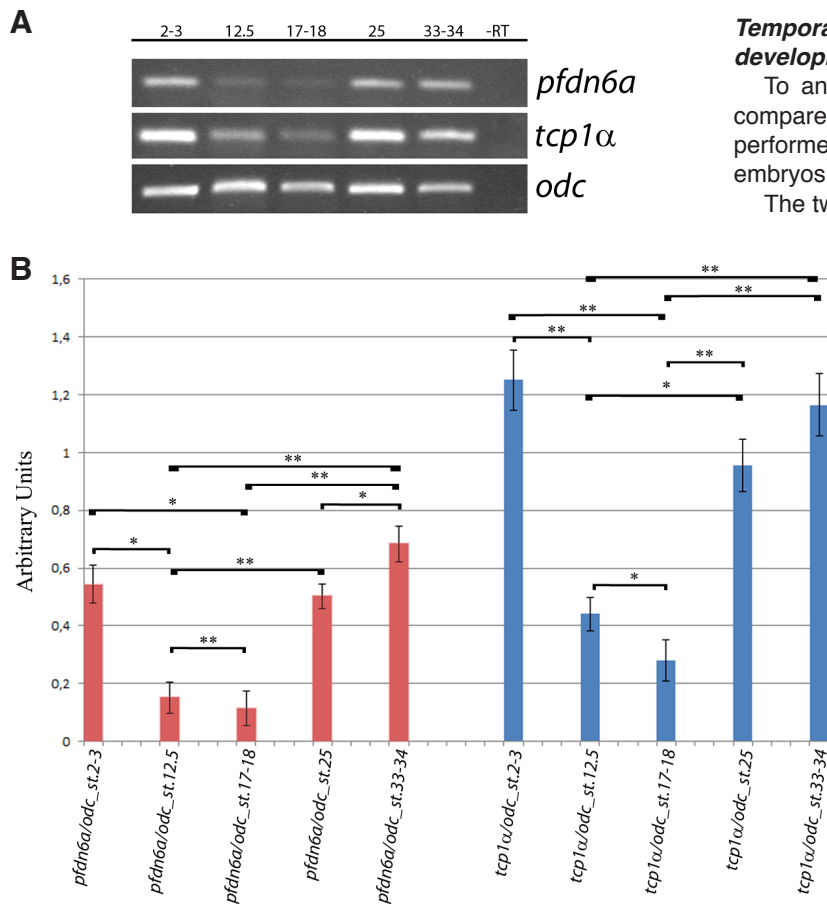
meiotic defects and resulting in morphological abnormalities and developmental lethality (Delgehr *et al.*, 2012). In addition, it is reported that the TCP1 complex is involved in cleavage furrow formation in *Drosophila* early embryos (Monzo *et al.*, 2010). The role of PFDN and TCP1 was also investigated in a few animal models of vertebrate development. PFDN1-deficient mice develop defective cytoskeletal function, loss of nerve bundles, hydrocephaly, neuromuscular defects, abnormal lymphocyte development and function, and a shortened life span (Lee *et al.*, 2011). Moreover, genetic disruption in the murine *Pfdn5* gene, leads to a reduction in formation of microtubules and microfilaments, resulting in progressive neurodegeneration, hydrocephalus and reproductive abnormalities, indicating that PFDN5 is required for normal sensory and neuronal development (Lee *et al.*, 2011). In zebrafish, a mutation in the  $\gamma$  subunit of TCP-1 was found to be responsible for the mutant *no tectal neuron* (*ntn*), which is characterized by defects in retinal ganglion cells differentiation and tectal neuropil formation, small pectoral fins and underdeveloped jaw skeletons (Matsuda and Mishina, 2004). In mouse, *tcp1 $\alpha$*  is observed at the morula and blastocyst stages and its expression is higher in post implantation embryos than in any adult organs except testis, indicating that *tcp1 $\alpha$*  expression is regulated spatially and temporally during embryogenesis (Kubota *et al.*, 1992). Finally, suppression of TCP1 activity in mouse photoreceptors leads to malformation of the outer segments and triggers retinal degeneration, indicating an essential role of TCP1 in the differentiation and survival of this photosensitive cell type (Sinha *et al.*, 2014).

Despite the pivotal role of amphibian models in understanding

vertebrate development, there are no data available about PFDN and little is known about TCP1 in these animal systems. To date, the only data reported on the amphibian homologue of TCP1 concern the expression of *tcp1 $\alpha$*  (CCT $\alpha$ ) in the axolotl (*Ambystoma mexicanum*), in which it is spatially and temporally regulated during neural and somitic development (Sun *et al.*, 1995), and the expression in *Xenopus laevis* embryos of *tcp1 $\alpha$*  and *tcp1 $\gamma$* , which appear to be developmentally regulated in neural-derived and myogenic lineages (Dunn and Mercola, 1996). Recently, we selected *pfdn6a* and *tcp1 $\alpha$*  in the course of a screen aimed at identifying genes coherently controlled by the retinal key regulator Rx1 (Giannaccini *et al.*, 2013; Giudetti *et al.*, 2014), consistently with previous data indicating a role of PFDN and TCP1 in retinal development (Matsuda and Mishina 2004; Lee *et al.*, 2011; Sinha *et al.*, 2014). The coregulation of these two genes by Rx1 suggested that they could display a general coordinated expression during embryogenesis. This prompted us to determine the spatio-temporal expression pattern of *pfdn6a*, which was not previously described, and compare it to the expression of *tcp1 $\alpha$* , extending the analysis to stages that, for the latter gene, had not been previously investigated.

## Results and Discussion

To provide novel insights into the regulation of *pfdn6a* we determined its spatio-temporal expression pattern during *Xenopus* development. Moreover, we performed a comparative analysis of *pfdn6a* and *tcp1 $\alpha$*  expression to evaluate the possible coregulation of these two genes.



### Temporal expression of *pfdn6a* and *tcp1 $\alpha$* during *Xenopus* development

To analyze the temporal expression pattern of *pfdn6a* and compare it to that of *tcp1 $\alpha$*  during embryonic development, we performed RT-PCR assays on cDNAs obtained from *Xenopus* embryos at different developmental stages.

The two genes display both maternal and zygotic expression, being detected before and after the midblastula transition (stage 8; Newport and Kirschner, 1982). They show a similar temporal expression profile, with their transcripts decreasing from the early blastomere stage to stage 18 and then increasing gradually from stage 25 to stage 33-34 (Fig. 1 A,B).

*tcp1 $\alpha$*  temporal expression pattern is consistent with that of the axolotl homologue, displaying maternal transcripts, detected in fertilized eggs, which are subsequently down-regulated in early gastrulae.

**Fig. 1.** RT-PCR analysis of *pfdn6a* and *tcp1 $\alpha$*  expression during *Xenopus* development. **(A)** *pfdn6a* and *tcp1 $\alpha$*  expression during embryonic development. cDNA derived from *Xenopus laevis* embryos at different stages (indicated at the top of the panel) was amplified using primers specific for *pfdn6a*, *tcp1 $\alpha$*  and ornithine decarboxylase gene (*odc*). The cDNAs were normalized to *odc*. For control reactions, reverse transcriptase was omitted (-RT). **(B)** Histogram representing the optical integrated density ratios of *pfdn6a*, *tcp1 $\alpha$*  and *odc* RT-PCR bands. The optical density was calculated using the ImageJ software. Values are means of 3 independent experiments. Significance: *p*-value < 0.05: \*; *p*-value < 0.01: \*\*.

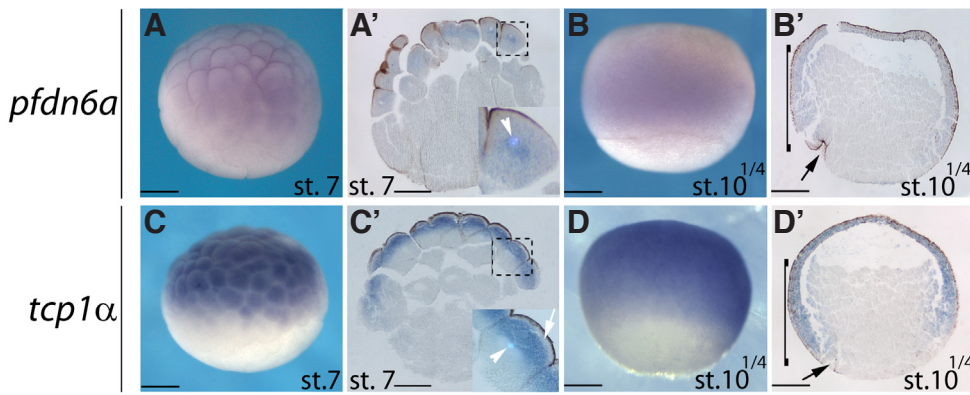


**Fig. 2.** Whole mount *in situ* hybridization analysis of *pdfn6a* and *tcp1α* during segmentation and gastrulation. Stages of embryos are indicated at the bottom right corner of each panel. (st.: stage), while the analyzed gene is indicated to the left of each row. (A,C) Lateral views of stage 7 embryos; animal pole to the top, vegetal pole to the bottom. (A', C') Sagittal sections of the hybridized embryos shown in (A) and (C), respectively; the insets in (A', C'), indicated by the dashed line square in each panel, show the intracellular localization of the two transcripts in animal blastomeres;

the white arrow in (C') shows absence of the *tcp1α* transcript in subcortical portion of cytoplasm; white arrowheads in (A', C') indicate Hoechst-stained nuclei. (B,D) Lateral view of stage 10<sup>1/4</sup> embryos; animal pole to the top, vegetal pole to the bottom. (B', D') Sagittal sections of the hybridized embryos shown in (B) and (D), respectively; black arrows point to the blastopore lip, square brackets indicate the involuting mesoderm. Scale bars, 250 μm.

Similarly, zygotic transcripts are mainly expressed in mid-neurula and later stage embryos (Sun *et al.*, 1995). On the other hand, in mouse, *tcp1* is expressed in post-implantation embryos and the amount of its mRNA decreases during development (from 7.5 to 17.5 day dpc) (Kubota *et al.*, 1992). Differences between amphibians and mouse in early *tcp1* expression may be ascribed to the possible lack of a maternal transcript in the mouse embryo, which is known to depend much less than amphibians on maternal RNAs stored in the oocyte. In addition, high levels of *tcp1* expression have been previously correlated with rapidly growing cells, which need to efficiently fold abundant proteins required for active growth (Kubota *et al.*, 1992). As the rate of early embryonic cell divisions is remarkably higher in amphibians than in mammals, this aspect may contribute to the observed expression differences.

Differently from *tcp1α*, the developmental expression of *pdfn6a* in Vertebrates has not been previously described.

**Spatial expression pattern of *pdfn6a* and *tcp1α* during *Xenopus* development**

Maternal transcripts of both genes are detected in the animal hemisphere during blastula stage (st.7) (Fig. 2 A,A',C,C'), with a different intracellular localization pattern: *pdfn6a* transcripts are mainly located in the perinuclear region (Fig. 2A', inset), while *tcp1α* is expressed in the apical portion of animal blastomeres except for the cytoplasmic subcortical region (Fig. 2C', inset). At early

gastrula stage (st. 10<sup>1/4</sup>) *pdfn6a* and *tcp1α* are both expressed in the ectoderm and in the presumptive mesoderm of the marginal zone (Fig. 2 B,B',D,D'). In particular, while sagittal sections of the hybridized embryos show a clear expression of *tcp1α* in the involuting mesoderm (Fig. 2 D,D' square bracket), *pdfn6a* appears to share a similar expression pattern although with a significantly lower hybridization signal (Fig. 2 B,B' square bracket).

Partially similar expression is observed in the axolotl where *tcp1α* transcript has been found localized along the blastopore at mid-gastrula stage (Sun *et al.*, 1995).

At neurula stages (st.13-19) *pdfn6a* and *tcp1α* are expressed in anterior and dorsal regions of the neural plate (Fig. 3 A,B,C,F,G, H). The presence of transcripts of both genes in migrating neural crests is visible in stage 16 and stage 19 embryos (Fig. 3 B,C,G,H white arrowheads). As expected from our previous microarray data (Giudetti *et al.*, 2014), we observed that Rx1 overexpression leads to the repression of both *pdfn6a* and *tcp1α* at stage 18/19 (Fig. 3D, I). As *Xenopus* development proceeds (st.22-23) the two genes are broadly expressed in the head, including eye anlagen and neural crests, as well as in dorsal and posterior region of the trunk (Fig. 3 E,J). As the expression of *tcp1α*, (alias *CCTa*) between stage 23 and 42 was previously reported (Dunn and Mercola, 1996) for these stages we mainly describe the expression of *pdfn6a*, except for those cases where a comparison with *tcp1α* is relevant.

In stage 27 embryos, a specific *pdfn6a* hybridization signal is

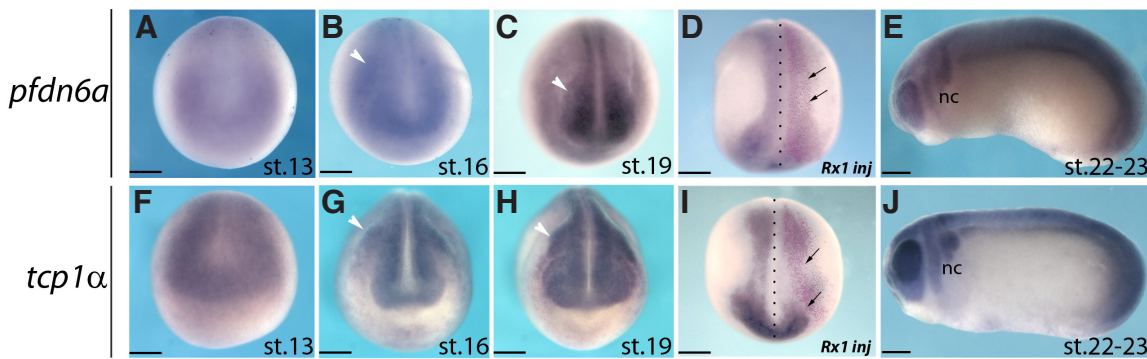
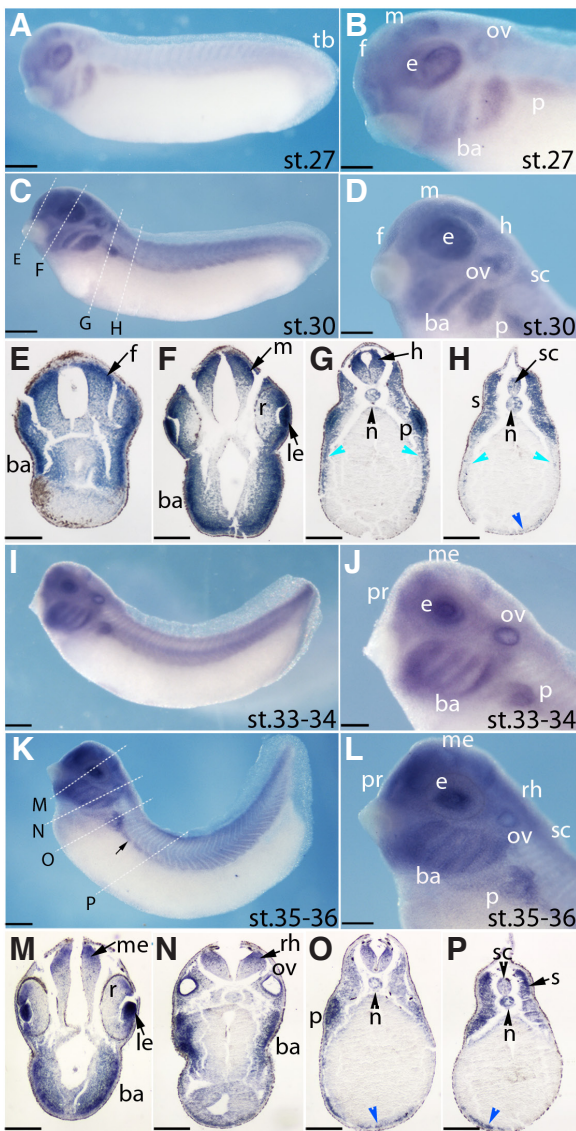


**Fig. 3.** Whole mount *in situ* hybridization analysis of *pdfn6a* and *tcp1α* during neurulation. (A-C, F-H) Frontal views (dorsal to the top) of hybridized embryos at the indicated neurula stages; white arrowheads indicate neural crests. (D, I) Dorsal view

of stage 18/19 embryos injected unilaterally with Rx1 RNA and nuclear LacZ RNA as a tracer (red staining). Arrows point at regions displaying stronger repression. (E, J) Lateral views of hybridized stage 22-23 embryos; anterior is to the left; nc: neural crests. Scale bars, 250 μm.



evident in forebrain, midbrain, eye vesicle, otic vesicle, branchial arches, anterior region of developing pronephros (Fig. 4 A,B). Somites show a *pfdn6a* signal progressively increasing towards tailbud region (Fig. 4A). In stage 30 embryos, *pfdn6a* extends its expression pattern to other regions of central nervous system such as hindbrain and spinal cord (Fig. 4 D,G,H). Moreover, sections of stage 30 hybridized embryos reveal that this gene is expressed in developing retina and lens anlagen (Fig. 4F), notochord (Fig. 4 G,H), lateral plate mesoderm (Fig. 4 G,H, light blue arrowheads). Furthermore, from stage 30 to later analyzed stages (st. 35-36), *pfdn6a* is expressed not only in the pronephric anterior region but also in the pronephric developing duct (Fig. 4 C,D,I-L).

The *pfdn6a* hybridization pattern observed in stage 30 embryos persists also at stage 33-34 and 35-36 (Fig. 4 I-L). In particular, sections of stage 35-36 embryos show higher levels of *pfdn6a* hybridization signal in dorsal region of mesencephalon and rhombencephalon (Fig. 4 M,N), retinal region and lens anlagen (Fig. 4M), branchial arches (Fig. 4M,N), otic vesicle (Fig. 4N), pronephros (Fig. 4O), notochord (Fig. 4 O,P) and spinal cord (Fig. 4P). From stage 30 to stage 35-36 *pfdn6a* is expressed in a ventral region of the embryos (Fig. 4 H,O,P, blue arrowheads).

As described by Dunn and Mercola (1996), we observed that *Xenopus tcp1α* is mainly expressed in neurogenic-derived, including developing cranial neural crest cells, and myogenic lineages

**Fig. 4 (left).** Whole mount *in situ* hybridization analysis of *pfdn6a* expression in tadpole embryos. Stages of embryos are indicated at the bottom right corner of each panel. (B,D,J,L) Magnified views of (A,C,I,K), respectively. In panels (A-D, I-L) anterior is to the left. Dashed lines in (C) point to the planes of the sections shown in (E-H). Dashed lines in (K) indicate the planes of the sections shown in (M-P). Light blue arrowheads in (G,H) point out a hybridization signal in lateral plate mesoderm at stage 30. Blue arrowheads point to *pfdn6a*-expressing ventral regions of stage 30 (H) and stage 35-36 embryos (O,P). Black arrow in (K) indicates pronephric developing duct. ba: branchial arches; e: eye; f: forebrain; h: hindbrain; le: lens; m: midbrain; me: mesencephalon; n: notochord; ov: otic vesicle; p: pronephros; pr: prosencephalon; rh: rhombencephalon; r: retina; s: somite; sc: spinal cord; tb: tailbud. Scale bars in (A, C, I, K), 500  $\mu$ m; in (B, D, J, L), 250  $\mu$ m; in (E-H, M-P), 200  $\mu$ m.

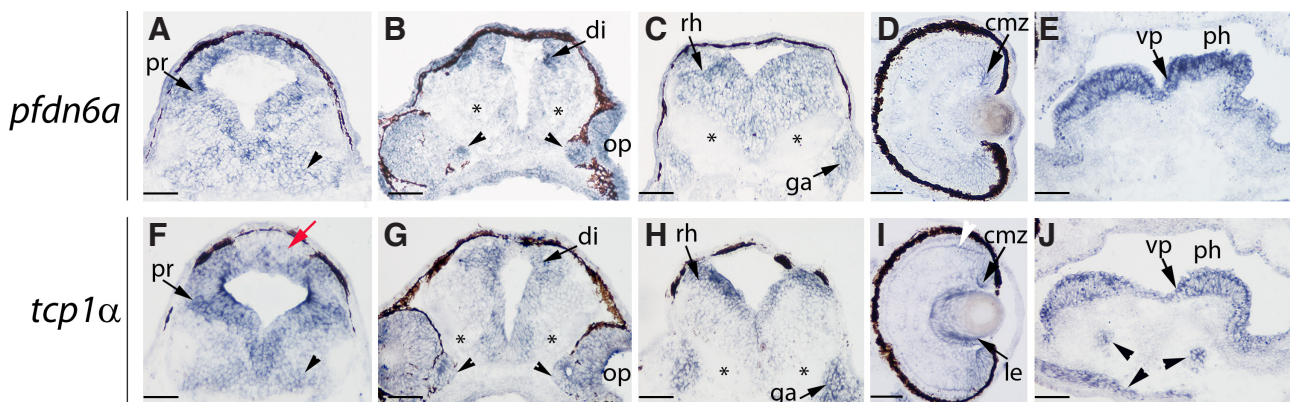


**Fig. 5.** Cryosections of stage 42 embryos hybridized with *pfdn6a* (A-E) and *tcp1α* probes (F-J). The red arrow in (F) denotes absence of *tcp1α* signal in a dorsal region of prosencephalon. Black arrowheads in (A,F) indicate a region located above the pharynx, labeled with *pfdn6a* and *tcp1α*, respectively. The asterisks in (B,C,G,H) indicate white matter at the level of diencephalon (B,G) and rhombencephalon (C,H). Black arrowheads in (B,G) indicate the Jacobson's organ. The white arrowhead in (I) points to the outer plexiform layer of retina. The black arrowheads in (J) indicate facial muscles. cmz: ciliary marginal zone; ga: ganglia; le: lens; op: olfactory pits; ph: pharynx; pr: prosencephalon; rh: rhombencephalon; vp: velar plate. Scale bars in (A-C, E, F-H, J), 100  $\mu$ m; in (D, I), 50  $\mu$ m.

(data not shown). In axolotl, the highest expression of *tcp1α* was detected in developing neural tissue, brain and somites in stage 16 (midneurula) until stage 43 (hatching) embryos (Sun *et al.*, 1995).

In parallel, a detailed comparison of the expression patterns of *pdfn6a* and *tcp1α* in anterior regions was performed on stage 42 embryos (Fig. 5). Hybridized cryostat sections show that both genes are expressed in prosencephalon, mesencephalon, rhombencephalon and cranial ganglia (Fig. 5 A-C,F-H), although *tcp1α* is not expressed in dorsal prosencephalic regions (Fig. 5F, red arrow). Conversely, the two genes are not expressed in white matter of diencephalon and rhombencephalon (Fig. 5 B,C,G,H, asterisks). In the eye, *tcp1α* is expressed in ciliary marginal zone (CMZ), outer plexiform layer (white arrowhead) and in cells of the proliferative layer of lens (Fig. 5I), while *pdfn6a* displays mainly a weak expression in the CMZ (Fig. 5D). Furthermore, both *pdfn6a* and *tcp1α* transcripts are detected in olfactory pits and Jacobson's organ (also known as vomeronasal organ) (Fig. 5 B,G, black arrowheads), which both constitute the larval olfactory organ of *Xenopus* (Hansen *et al.*, 1998). Finally, the transcripts of both genes have been detected in head regions located between prosencephalon and pharynx (Fig. 5A, F, black arrowheads), and in velar plate of the mouth located in ventral oral endoderm (Fig. 5 E,J). However, we observed that *pdfn6a* transcripts are not found in some facial muscles underlying the pharynx that express *tcp1α* (Fig. 5 E,J; Dunn and Mercola, 1996)

In conclusion, we found that both *pdfn6a* and *tcp1α* are spatially and temporally regulated during embryogenesis of *Xenopus*. Moreover, their transcripts show many sites of coexpression in embryos at different developmental stages, suggesting that both genes share a common transcriptional regulation and could be involved in the same developmental events.

## Materials and Methods

### RNA extraction and RT-PCR analysis

Total RNA was extracted from different embryonic stages by using Mini RNA Isolation Kit (Nucleospin RNA XS, Macherey Nagel). First strand cDNA was synthesized using Superscript II Reverse Transcriptase (Invitrogen), from 1 µg of total RNA. RT-PCR analysis was performed using gene-specific sets of primers:

*tcp1α*-forward: 5'-AGTCTGTCGTACCCGGAGGT-3'  
*tcp1α*-reverse: 5'-AGCATTACCCGCTAGGGTTT-3'  
*pdfn6a*-forward: 5'-CCGAGATTGCCAATACCAG-3'  
*pdfn6a*-reverse: 5'-ACTGAGCCTCAAGCTTTTGC-3'  
*odc*-forward: 5'-GGGCTGGATCGTATCGTAGA-3'  
*odc*-reverse: 5'-CTTCAGGGAGAATGCCATGT-3'

### In situ hybridization and microinjections

*Xenopus* embryos were staged according to Nieuwkoop and Faber (1967).

Whole-mount *in situ* hybridization was performed according to standard protocols (Harland *et al.*, 1991) with minor modifications (see Marracci *et al.*, 2013). Probes for *pdfn6a* and *tcp1α* were transcribed from cDNA clones AGENCOURT\_11041475 (GenBank Acc. no. CA988538.1) and XL418a19ex (GenBank Acc. no. BP674881), respectively.

Antisense transcripts were prepared by plasmid linearization with Sall (*pdfn6a*) or BamHI (*tcp1α*) and *in vitro* transcription using T7 and T3 RNA polymerase (Roche), respectively. Sense transcripts were used as negative control (data not shown).

For *in situ* hybridization on cryostat sections (12 µm), embryos were fixed and cryoprotected following the experimental procedure previously described (D'Autilia *et al.*, 2010; Marracci *et al.*, 2011).

Rx1 and nuclear-LacZ were microinjected in one dorsal blastomere at four-cell stage, as previously described (Giudetti *et al.*, 2014).

### Paraffin sectioning

Whole-mount hybridized embryos were paraffin-embedded and cut at a thickness of 15-29 µm with a Reichert-Jung Autocut 2040 Microtome. After Hoechst-counterstaining, the sections were washed and mounted in Aqua Poly/Mount (Polysciences Inc.).

### Acknowledgements

We are grateful to Naoto Ueno, for generously providing the XL418a19ex plasmid, and thank Marzia Fabbri, Donatella De Matienzo and Elena Landi for technical assistance, and Salvatore Di Maria for frog care.

## References

- D'AUTILIA S, BROCCOLI V, BARSACCHI G, ANDREAZZOLI M (2010). *Xenopus* Bsx links daily cell cycle rhythms and pineal photoreceptor fate. *Proc Natl Acad Sci USA* 107: 6352–6357.
- DELGEHYR N, WIELAND U, RANGONE H, PINSON X, MAO G, DZHINDZHEV NS, MCLEAN D, RIPARBELLI MG, LLAMAZARES S, CALLAINI G, GONZALEZ C, GLOVER DM (2012). *Drosophila* Mgr, a Prefoldin subunit cooperating with von Hippel Lindau to regulate tubulin stability. *Proc Natl Acad Sci USA* 109: 5729–5734.
- DUNN M, MERCOLA M (1996). Cloning and Expression of *Xenopus* CCTgamma, a Chaperonin Subunit Developmentally Regulated in Neural-Derived and Myogenic Lineages *Dev Dyn* 205: 387–394.
- GIANNACCINI M, GIUDETTI G, BIASCI D, MARIOTTI S, MARTINI D, BARSACCHI G, ANDREAZZOLI M (2013). Rx1 defines retinal precursor identity by repressing alternative fates through the activation of TLE2 and Hes4. *Stem Cells* 31: 2842–2847.
- GIUDETTI G, GIANNACCINI M, BIASCI D, MARIOTTI S, DEGL'INNOCENTI A, PERROTTA M, BARSACCHI G, ANDREAZZOLI M (2014). Characterization of the Rx1-dependent transcriptome during early retinal development. *Dev Dyn* 243: 1352–1361.
- HANSEN W J, COWAN N J, WELCH W J (1999). Prefoldin-nascent chain complexes in the folding of cytoskeletal proteins. *J Cell Biol* 145: 265–77.
- HARLAND R M (1991). *In situ* hybridization: an improved whole-mount method for *Xenopus* embryos. *Methods Cell Biol* 36: 685–95.
- KUBOTA H, WILLISON K, ASHWORTH A, NOZAKI M, MIYAMOTO H, YAMAMOTO H, MATSUSHIRO A, MORITA T (1992). Structure and expression of the gene encoding mouse t-complex polypeptide (Tc-1). *Gene* 120:207–215.
- LEE Y, SMITH R S, JORDAN W, KING B L, WON J, VALPUESTA J M, NAGGERT J K, NISHINA P M (2011). Prefoldin 5 is required for normal sensory and neuronal development in a murine model. *J Biol Chem* 286: 726–736
- MARRACCI S, MICHELOTTI V, CASOLA C, GIACOMA C, RAGGHIANI M (2011). *Daz*- and *Pumilio*-like genes are asymmetrically localized in *Pelophylax* (*Rana*) oocytes and are expressed during early spermatogenesis. *J Exp Zool (Mol Dev Evol)* 316:330–338.
- MARRACCI S, GIANNINI M, VITIELLO M, ANDREAZZOLI M, DENTE L (2013). *Kidins220/ARMS* is dynamically expressed during *Xenopus laevis* development *Int J Dev Biol* 57: 787–792.
- MARTÍN-BENITO J, BOSKOVIC J, GÓMEZ-PUERTAS P, CARRASCOSA J L, SIMONS C T, LEWIS S A, BARTOLINI F, COWAN N J, VALPUESTA J M (2002). Structure of eukaryotic prefoldin and of its complexes with unfolded actin and the cytosolic chaperonin CCT. *EMBO J* 21:6377–6386.
- MATSUDA N, MISHINA M. (2004). Identification of chaperonin CCT gamma subunit as a determinant of retinotectal development by whole-genome subtraction cloning from zebrafish no tectal neuron mutant. *Development* 131:1913–1925.
- MILLÁN-ZAMBRANO G, CHÁVEZ S (2014). Nuclear functions of prefoldin. *Open Biol* 4. pii: 140085. doi: 10.1098/rsob.140085.
- MONZO K, DOWD S R, MINDEN J S, SISSON J C (2010). Proteomic analysis reveals CCT is a target of Fragile X mental retardation protein regulation in *Drosophila*. *Dev Biol* 340:408–418.
- NEWPORT J, KIRSCHNER M (1982). A major developmental transition in early *Xenopus* embryos: II. Control of the onset of transcription. *Cell* 30: 687–696.
- NIEUWKOOP P D, FABER J (1967). Normal Table of *Xenopus laevis*. Amsterdam,

The Netherlands: North Holland Publishing Company.

PEJANOVIC N, HOCHRAINER K, LIU T, AERNE B L, SOARES M P, ANRATHER J (2012). Regulation of nuclear factor  $\kappa$ B (NF- $\kappa$ B) transcriptional activity via p65 acetylation by the chaperonin containing TCP1 (CCT). *PLoS One* 7:e42020.

SINHA S, BELCASTRO M, DATTA P, SEO S, SOKOLOV M (2014). Essential role of the chaperonin CCT in rod outer segment biogenesis. *Invest Ophthalmol Vis Sci* 55: 3775-3785.

SÖNNICHSEN B, KOSKI L B, WALSH A, MARSCHALL P, NEUMANN B, BREHM M, ALLEAUME A M, ARTELT J, BETTENCOURT P, CASSIN E, et al. (2005). Full-genome RNAi profiling of early embryogenesis in *Caenorhabditis elegans*. *Nature* 434: 462-469.

SUN H B, NEFF A W, MESCHER A L, MALACINSKI G M (1995). Expression of the axolotl homologue of mouse chaperonin t-complex protein-1 during early development. *Biochim Biophys Acta* 1260:157-166.

### Further Related Reading, published previously in the *Int. J. Dev. Biol.*

#### **Kidins220/ARMS is dynamically expressed during *Xenopus laevis* development**

Silvia Marracci, Marianna Giannini, Marianna Vitiello, Massimiliano Andreazzoli and Luciana Dente  
*Int. J. Dev. Biol.* (2013) 57: 787-792  
<http://dx.doi.org/10.1387/ijdb.130080sm>

#### **Dicer inactivation causes heterochronic retinogenesis in *Xenopus laevis***

Sarah Decembrini, Massimiliano Andreazzoli, Giuseppina Barsacchi and Federico Cremisi  
*Int. J. Dev. Biol.* (2008) 52: 1099-1103  
<http://dx.doi.org/10.1387/ijdb.082646sd>

#### **The *Xenopus* ortholog of the nuclear hormone receptor *Nr2e3* is primarily expressed in developing photoreceptors**

Reyna I. Martinez-De Luna and Heithem M. El-Hodiri  
*Int. J. Dev. Biol.* (2007) 51: 235-240  
<http://dx.doi.org/10.1387/ijdb.062236rm>

#### **Retinal stem cells in vertebrates: parallels and divergences**

Marcos A. Amato, Emilie Arnault and Muriel Perron  
*Int. J. Dev. Biol.* (2004) 48: 993-1001  
<http://dx.doi.org/10.1387/ijdb.041879ma>

#### **Regulation of vertebrate eye development by *Rx* genes**

Travis J. Bailey, Heithem El-Hodiri, Li Zhang, Rina Shah, Peter H. Mathers and Milan Jamrich  
*Int. J. Dev. Biol.* (2004) 48: 761-770  
<http://dx.doi.org/10.1387/ijdb.041878tb>

5 yr ISI Impact Factor (2013) = 2.879

